Supplementary Information for

Electron Correlation and Incipient Flat Bands in the Kagome Superconductor $CsCr_3Sb_5$

Yidian Li[1*], Yi Liu[2,3*], Xian Du[1*], Siqi Wu[2], Wenxuan Zhao[1], Kaiyi Zhai[1], Yinqi Hu[1], Senyao Zhang[1], Houke Chen[4], Jieyi Liu[4], Yiheng Yang[4], Cheng Peng[4], Makoto Hashimoto[5], Donghui Lu[5], Zhongkai Liu[6,7], Yilin Wang[8,9†], Yulin Chen[4,6,7†], Guanghan Cao[2†], and Lexian Yang[1,10†]

[1]*State Key Laboratory of Low Dimensional Quantum Physics, Department of Physics, Tsinghua University, Beijing 100084, China.*

[2]*School of Physics, Zhejiang University, Hangzhou 310058, China*

[3]*Department of Applied Physics, Key Laboratory of Quantum Precision Measurement of Zhejiang Province, Zhejiang University of Technology, Hangzhou 310023, China*

[4]*Department of Physics, Clarendon Laboratory, University of Oxford, Parks Road, Oxford OX1 3PU, UK.*

[5]*Stanford Synchrotron Radiation Lightsource, SLAC National Accelerator Laboratory, Menlo Park, CA 94025, USA*

[6]*School of Physical Science and Technology, ShanghaiTech University and CAS-Shanghai Science Research Center, Shanghai 201210, China.*

[7]*ShanghaiTech Laboratory for Topological Physics, Shanghai 200031, China.*

[8]*School of Emerging Technology, University of Science and Technology of China, Hefei 230026, China*

[9]*New Cornerstone Science Laboratory, University of Science and Technology of China, Hefei 230026, China*

[10]*Collaborative Innovation Center of Quantum Matter, Beijing 100084, China.*

*These authors contributed equally to this work.

†e-mail: YLW: yilinwang@ustc.edu.cn; YLC: yulin.chen@physics.ox.ac.uk; GHC: ghcao@zju.edu.cn; LXY: lxyang@tsinghua.edu.cn.

This file contains the following contents:

I. Comparison between *ab-initio* calculations with and without spin-orbit coupling.

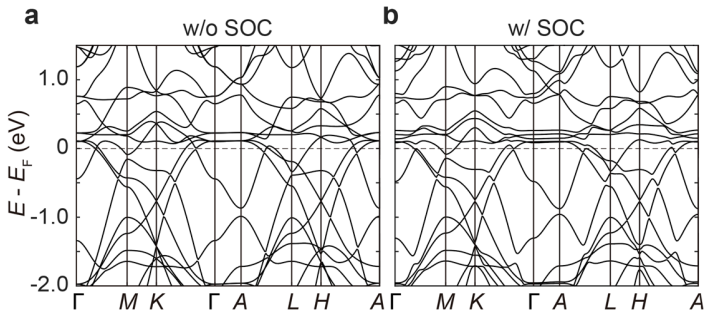

Supplementary FIG. 1 | Comparison between *ab-initio* calculations (**a**) with and (**b**) without spin-orbit coupling (SOC).

Supplementary Figure 1 compares the *ab-initio* calculated band structure of $CsCr_3Sb_5$ with and without spin-orbit coupling (SOC). In general, the SOC effect induces minor changes in the occupied part of the band structure, except the gap at the Dirac points at the *K* and *H* points. Remarkably, it splits the flat band just above E_F, which may provide a method to tune the flat bands in $CsCr_3Sb_5$ through element substitution.

II. Single crystal X-ray diffraction measurements of $CsCr_3Sb_5$.

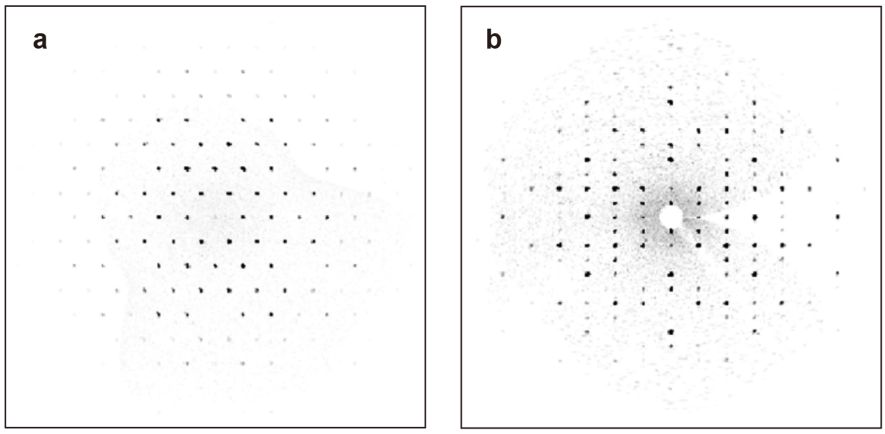

Supplementary FIG. 2 | Single crystal X-ray diffraction (XRD) of $CsCr_3Sb_5$. Patterns were measured along the (**a**) (hk2) plane, and (**b**) (0kl) plane. Data were collected at the room temperature.

In Supplementary Figure 2, we show the XRD experiments of $CsCr_3Sb_5$. which reveals shape diffraction peaks and confirms the high quality of the samples in our experiment.

III. Core-level spectra of $CsCr_3Sb_5$.

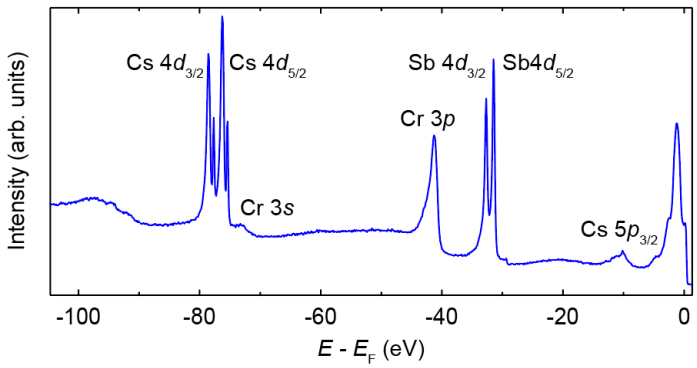

Supplementary FIG. 3 | Core energy levels of $CsCr_3Sb_5$. Data were measured with 160 eV photons.

Supplementary Figure 3 shows the core-level spectra of $CsCr_3Sb_5$. We observe sharp peaks from Cs, Cr, and Sb core levels, confirming the composition of our samples. We notice two sets of Cs peaks around the binding energy of 78 eV, resembling the results in CsV_3Sb_5, which were attributed to the different chemical environments of Cs atoms after cleavage [1].

IV. Band structure measured at different photon energies.

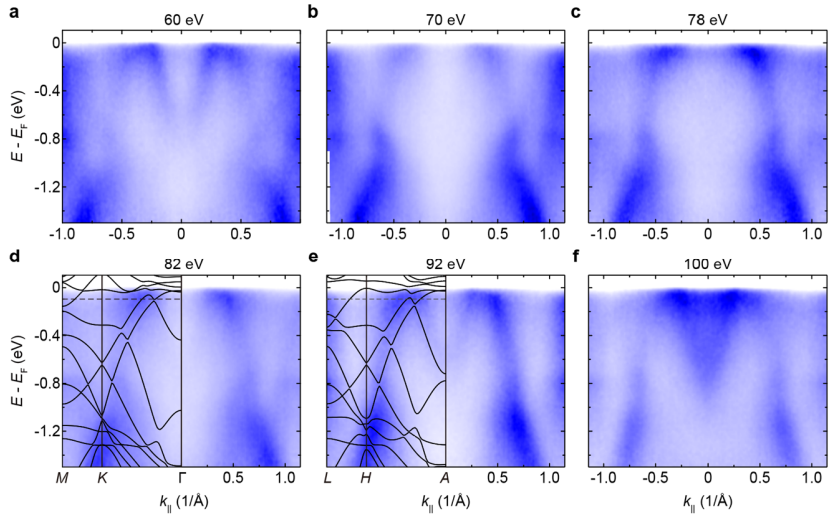

Supplementary FIG. 4 | Band structure along the $\bar{\Gamma}$-$\bar{K}$ direction measured at different photon energies. Data collected using linear-horizontally (LH) and linear-vertically (LV) polarized photons are merged for completeness of the electronic structure. The calculated band structure (black solid

lines) is renormalized by a factor of 1.4 and shifted by 100 meV for comparison with experiments in (**d**) and (**e**).

Supplementary Figure 4 shows the band structure measured at different photon energies. The band dispersions are generally similar to each other, suggesting a weak k_z variation of the band structure. The comparison between our experiments and calculated results suggests that the strong electronic correlation shows a minor impact on the Sb *p* orbital bands but strongly broadens Cr *d* orbital bands.

V. Comparison between experimental and calculated band structure.

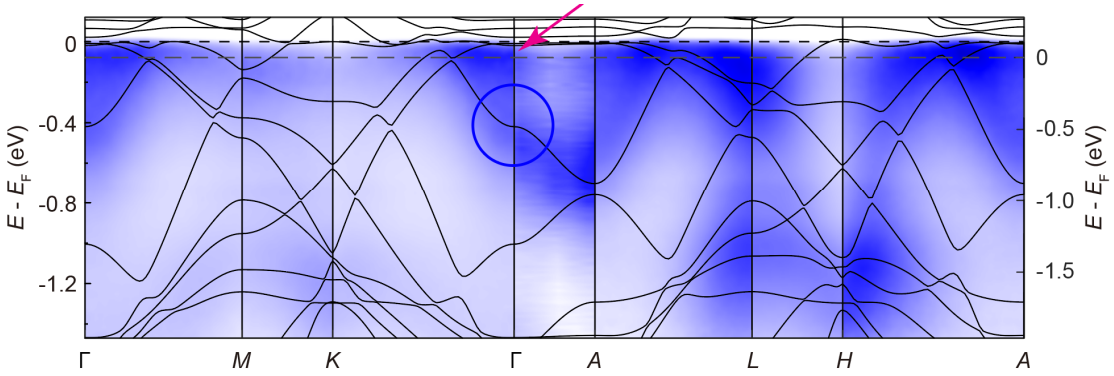

Supplementary FIG. 5 | Fine experimental band dispersions of $CsCr_3Sb_5$ overlaid with the calculated band structure. The red arrow indicates the flat band close to E_F and the blue circle indicates the van Hove singularity (vHS) at the Γ point.

Supplementary Figure 5 compares the fine electronic structure along high-symmetry directions near E_F (left vertical axis) and the calculated results (right vertical axis). The direct comparison suggests that the experimental data are in overall agreement with the calculation after renormalized by a factor of 1.4 and shifts downward by about 100 meV (or equivalently, the calculated Fermi level is raised up by about 100 meV). With the help of the calculation, we can resolve the flat band and the van Hove Singularity (vHS) at the Γ point.

VI. Laser-ARPES data at high temperature divided by the Fermi-Dirac distribution function.

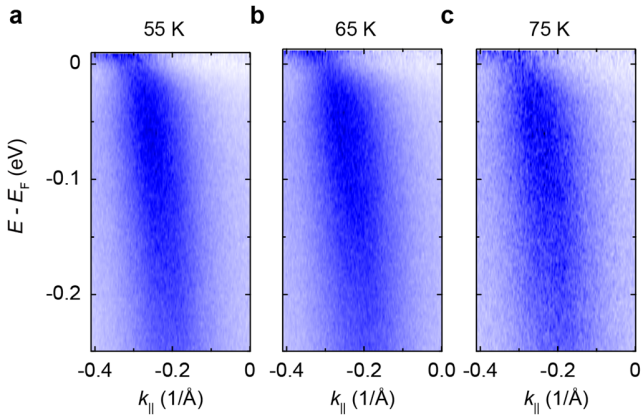

Supplementary FIG. 6 | Laser-ARPES data at **a,** 55 K, **b,** 65 K, and **c,** 75 K divided by the Fermi-Dirac distribution function. Data were measured with LV-polarized photons.

Supplementary Figure 6 shows the laser-ARPES data divided by the Fermi-Dirac (FD) distribution function at high temperatures. The electron band tends to be flattened as approaching E_F and exhibits a gap-like feature near E_F, which agrees with the calculation in Supplementary Fig. 1b.

VII. Orbital-projected calculation of the band structure.

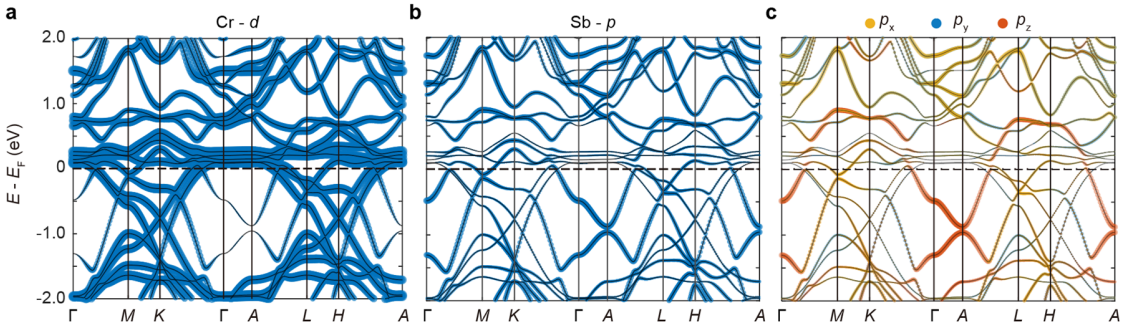

Supplementary FIG. 7 | Calculated band structure projected onto **a,** Cr *d* orbtials, **b,** Sb *p* orbitals, and **c,** Sb *p* orbital components.

In Fig. 3a of the main text, we show the band structure projected onto the Cr 3*d* orbitals. Supplementary Figure 7 further shows the band structure projected onto (a) Cr *d*, (b) Sb *p*, and (c) Sb *p* orbital components. The bands near E_F are mostly composed of Cr *d* orbitals hybridizing with Sb *p* atom orbitals. In our ARPES experiments, the electron band around $\bar{\Gamma}$ near E_F from Sb *p* orbital is clearly resolved, while the Cr *d* orbital bands show broadened spectra due to the strong correlation effect (see the main text). We notice that the electron band around $\bar{\Gamma}$ has mixed *d* orbital

component, suggesting a *p-d* interaction, which accounts for the renormalization of this band (Supplementary Fig. 5).

VIII. Flat band dispersion along the Γ*K* direction.

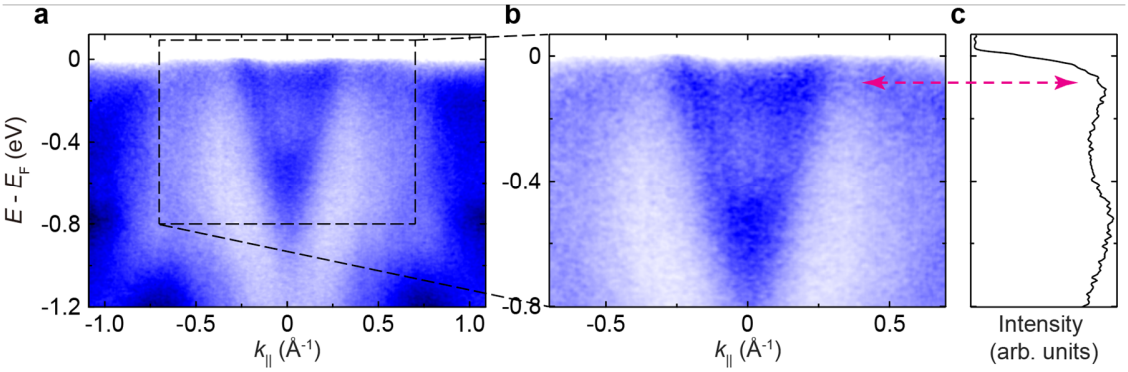

Supplementary FIG. 8 | Flat band measured along the Γ*K* direction. **a-b,** ARPES spectrum and its zoom-in plot as indicated by the dashed rectangle. **c,** the corresponding energy distribution curve (EDC) at the Γ point. The red dashed arrow indicates the flat band. Data were measured with 62 eV photons.

In Fig. 3d of the main text we show the flat band observed along the *AH* direction. In Supplementary Figure 8, we further show the observation of the flat band along the Γ*K* direction, which is supported by the peak in the energy distribution curve (EDC) at Γ (Supplementary Fig. 8c).

IX. DFT+DMFT calculation of the electronic structure with different Hund's coupling.

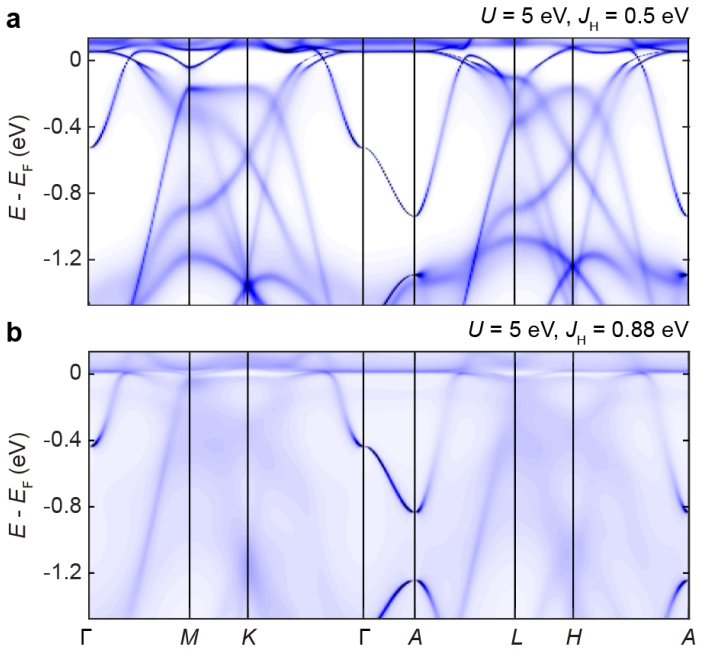

Supplementary FIG. 9 | DFT+DMFT calculation of the electronic structure, with (**a**) on-site Coulomb interaction $U = 5$ eV, Hund's coupling $J_H = 0.5$ eV, and (**b**) $U = 5$ eV, $J_H = 0.88$ eV. The calculations were conducted with the temperature parameter $T = 100$ K.

Supplementary Fig. 9 compares the DFT+DMFT calculation of the electronic structure with the same on-site Coulomb interaction U but different Hund's coupling J_H. Compared with the DFT calculation in the main text, the band structure is not strongly renormalized by U. The Hund's coupling greatly enhances electron self-energy and induces intrinsically incoherent Cr 3*d* states. Consistent with our ARPES experiment, we concluded that a large J_H (> 0.5 eV) is required to properly describe the band structure of $CsCr_3Sb_5$.

X. DFT+DMFT calculation of the electronic structure at different temperatures.

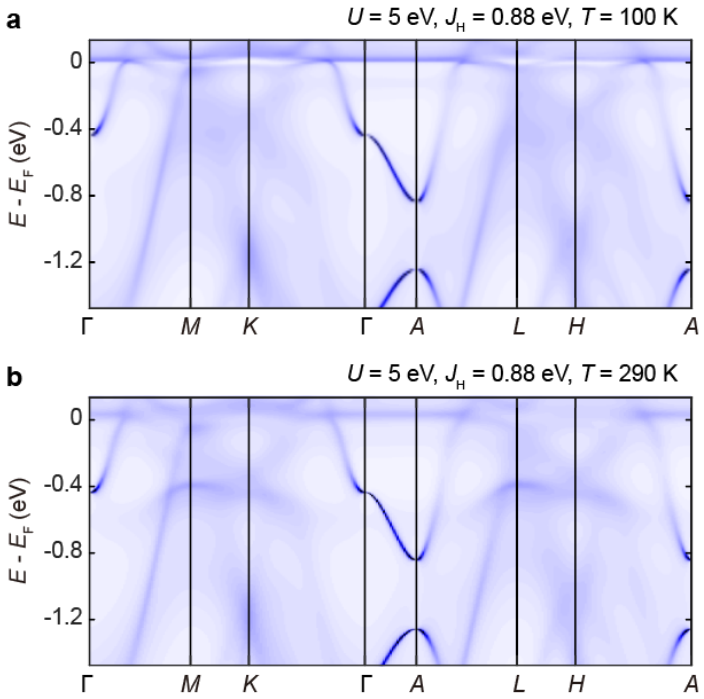

Supplementary FIG. 10 | DFT+DMFT calculation of the electronic structure, with (**a**) on-site Coulomb interaction $U = 5$ eV, Hund's coupling $J_H = 0.5$ eV, temperature $T = 100$ K, and (**b**) $U = 5$ eV, $J_H = 0.88$ eV, $T = 290$ K.

Hund's correlation leads to incoherent spectra at high temperatures due to strong fluctuations of local Cr 3*d* moments. As the temperature decreases, the system is expected to undergo an incoherence-to-coherence crossover by screening the local moments. Therefore, the relatively coherent flat bands can be observed near E_F, as shown in the DMFT calculations at different temperatures in Supplementary Figure 10.

XI. Flat band measured with photons at 200 eV.

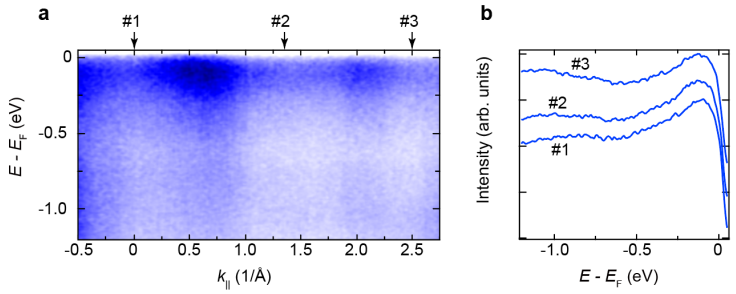

Supplementary FIG. 11 | Observation of the flat band using photons at 200 eV. **a**, ARPES intensity map along $\bar{\Gamma}\bar{M}$. **b**, EDCs at the momentum positions marked in **a**. The flat band can be resolved directly in the ARPES intensity map and EDC peaks.

In Supplementary Figure 11, we show the flat band along the $\bar{\Gamma}\bar{M}$ direction can be clearly resolved using photons at 200 eV, which are supported by the peaks in the EDCs at three selected $k_{\|}$ positions.

XII. Temperature-dependence of the flat band.

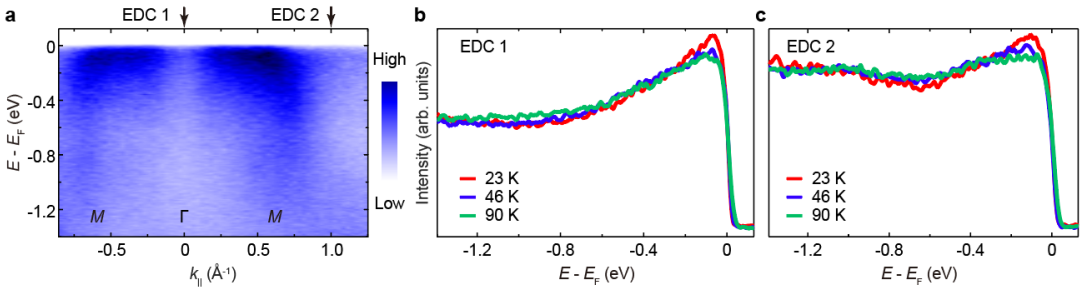

Supplementary FIG. 12 | Temperature-dependent band dispersion along the Γ*M* direction. **a**, Band structure along the Γ*M* direction. **b**, **c**, Temperature-dependent energy-distribution curves (EDCs) at (**b**) the Γ point (EDC 1) and (**c**) $k_{\|}$ = 1.0 Å^{-1} (EDC 2). Data were collected using linear-vertically (LV) polarized photons at 62 eV.

In Supplementary Figure 12, we show temperature-dependent experiments across the density-wave transition. We do not observe a clear change of the flat band position, except for a slight suppression of its spectral weight.

References:

1. Kato T, *et al.* Polarity-dependent charge density wave in the kagome superconductor CsV_3Sb_5. *Phys. Rev. B* **106**, L121112 (2022).